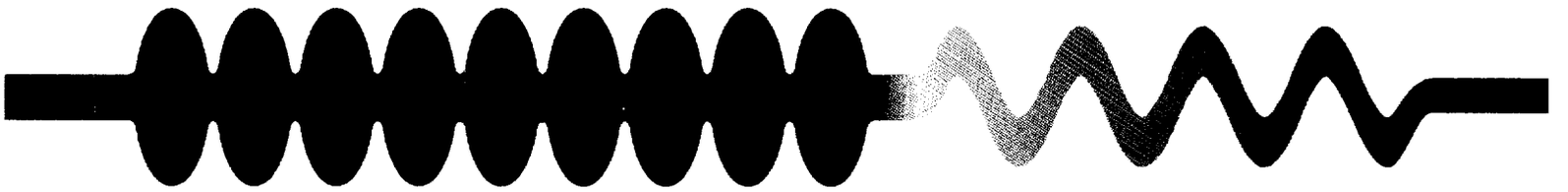

Regenerative FEL Amplifier at the DESY TESLA Test Facility as a Fully Coherent VUV Laser

B. Faatz, J. Feldhaus, J. Krzywinski*, E.L. Saldin+,
E.A. Schneidmiller+, M.V. Yurkov°

HASYLAB-DESY, *Institute of Physics, Warszawa,
+ASC Samara, °JINR Dubna

November 1997, TESLA-FEL 97-07

TESLA FEL Reports are available from:

Deutsches Elektronen-Synchrotron DESY
MHF-SL Group
Katrin Lando
Notkestraße 85
22603 Hamburg
FRG

Phone: (0049/40) 8998 3339
Fax: (0049/40) 8998 4302
e-mail: lando@lando.desy.de or landok@vxdesy.desy.de

Regenerative FEL Amplifier at the DESY TESLA Test Facility as a Fully Coherent VUV Laser

B. Faatz [a], J. Feldhaus [a], J. Krzywinski [b], E.L. Saldin [c], E.A. Schneidmiller [c], M.V. Yurkov [d]

[a] *Hamburger Synchrotronstrahlungslabor(HASYLAB) at Deutsches Electronen-Synchrotron(DESY), Notkestrasse 85, D-22607 Hamburg, Germany*

[b] *Institute of Physics of the Polish Academy of Sciences, 02688 Warszawa, Poland*

[c] *Automatic Systems Corporation, 443050 Samara, Russia*

[d] *Joint Institute for Nuclear Research, Dubna, 141980 Moscow Region, Russia*

Abstract

The paper presents a conceptual design of a regenerative FEL amplifier (RAFEL) as an extension of the single-pass free electron laser project at the TESLA Test Facility (TTF) at DESY. The proposed scheme requires the additional installation of only three optical components for a narrow-band feedback system and is fully compatible with the present design and the infrastructure developed for the TTF FEL project. It would allow to construct a tunable VUV laser with a minimum wavelength around 60 nm, a pulse duration of 1 ps, a peak power of about 300 MW and an average power of about 30 W. The output radiation of the regenerative FEL amplifier would possess all the features which are usually associated with laser radiation: full transverse and longitudinal coherence and shot-to-shot stability of the output power. The degeneracy parameter of the output radiation would be about 10^{14} and thus have the same order of magnitude as that of a quantum laser operating in the visible.

November 1997, TESLA-FEL 97-07

1 Introduction

Free-electron laser techniques provide the possibility to extend the energy range of lasers into the vacuum ultra-violet (VUV) and X-ray regime using a single-pass free electron laser (FEL) amplifier based on the self-amplification of spontaneous emission (SASE). One particular feature of the FEL amplifier is its rather large amplification bandwidth. When the process of amplification starts from noise, it produces a relatively wide-band spectrum of output radiation with only a short length of longitudinal coherence. For instance, the bandwidth of the VUV SASE FEL at DESY would be about one per cent at 70 nm. The output radiation consists of a number of independent wavepackets (or spikes). As a rule, the length of each wavepacket is much less than the radiation pulse length and there is no phase correlation between the wavepackets. Therefore, the improvement of the longitudinal coherence of VUV and X-ray FELs is of great practical importance.

At present two ways to overcome this problem are under study at DESY. The first one is based on the idea to use a two-stage single-pass FEL amplifier [1–3]. The FEL consists of two undulators and a grazing-incidence monochromator located between them. Since it is a single bunch scheme, it does not require any special time diagram for the accelerator operation and is not affected by any time jitter of the electron pulses in the train. Another approach is based on the idea to employ a narrow-band feedback between exit and entrance of the FEL operating in a multibunch mode [4,5]. When the first electron bunch passes the undulator, it amplifies shot noise and produces powerful, but wide-band radiation. At the exit of the undulator a small fraction of the output radiation is reflected into a monochromator selecting a narrow band of radiation which is then returned to and focused on the entrance of the undulator. If the monochromatic radiation power is significantly higher than that of the shot noise, the second electron bunch (and all others in the bunch train) amplifies this narrow band of radiation. For the narrow-band monochromator in the feedback it has been proposed to use diffraction from atomic lattices for a soft X-ray FEL [5] or Bragg reflection from single crystals for the Å wavelength regime [4]. In the VUV high reflectivity can be obtained from mirrors and gratings near normal incidence, greatly simplifying the design of a feedback system.

In the first stage (Phase I) of the SASE FEL project at the TESLA Test Facility (TTF) at DESY the linear accelerator will operate at electron beam energies up to 390 MeV and will allow to reach wavelengths down to approximately 40 nm [6]. Phase I is intended to test various novel hardware components and to prove the SASE principle for the first time at short wavelengths. The technical parameters of the facility which is

presently under construction are such that it can be easily extended by a narrow-band optical feedback system turning the single-pass SASE FEL starting from noise into a regenerative FEL amplifier (RAFEL) [7] providing for the first time fully coherent, powerful VUV laser radiation continuously tunable between approximately 200 nm and 60 nm.

2 Design of the narrow-band feedback

The main goal of the present study has been to design a RAFEL scheme which is compatible with the layout of the TTF and the VUV SASE FEL under construction at DESY, and which can be realized with minimal additional effort. The optical system proposed can be installed in the unoccupied straight vacuum line bypassing the magnetic chicane used to compress the electron bunches ("second bunch compressor"), and in the experimental area reserved for photon diagnostics, behind the dipole magnet separating the electron beam from the photon beam. The distance between these two areas is just about twice the distance between two electron pulses (2×33.3 m $=$ 66.6 m) providing natural synchronization of electron and photon pulses without any additional optical delay line.

The schematic layout of the feedback system adopted to the TTF site is shown in Fig. 1. Detailed drawings of the experimental area and the bunch compressor area with the optical elements of the feedback system are presented in Figs. 2 and 3, respectively. The optical design is based on an autocollimating scheme and requires only three optical elements: two spherical mirrors, M_1 and M_2, and a plane blazed grating in the so-called Littrow mounting [8] (see Fig. 1). In order to make use of the FEL output radiation an additional mirror is needed to couple out the major fraction of the radiation power (90 %) and to direct it to the experimental area. A central hole in this mirror transmits approximately 10 % of the radiation power which is collected by the mirror M_1 placed 1 m behind it and reflected back into itself towards the monochromator. The radius of mirror M_1 has been chosen as to produce a plane reflected wavefront.

The minimum size of the hole in the outcoupling mirror is defined by the condition that radiation losses due to aperture limitations in the optical feedback system should be avoided. The smallest aperture in the beamline has a diameter of 8 mm (the electron beam collimator located in front of the undulator). Since amplitude and phase variation of the radiation across the mirror hole is small, the far field diffraction pattern is given by the Fraunhofer diffraction formula for a uniform circular aperture. The central bright spot is known as the Airy disk, and the radii of the rings are defined by the

zero values of the Bessel function $J_1(x)$ with $x = \frac{\pi}{\lambda} D sin\theta$. The size of the Airy disk at the position of the electron beam collimator should be equal to the diameter of the collimator D_c (see Fig. 4):

$$2.44\frac{\lambda}{D} = \frac{D_c}{L},$$

where L is the distance between the hole and the collimator and λ is the radiation wavelength. In the present design $D_c = 8$ mm and $L = 30$ m. Hence the diameter of the hole should be $D \simeq 10^4\lambda$, i.e. $D \simeq 1.2$ mm for a wavelength $\lambda = 120$ nm. The fraction of the FEL output power passing the mirror hole is then calculated from the angular distribution of the output radiation power from the undulator (see Fig. 5). At the mirror-to-undulator distance of 14 m the fraction of the output power directed into the feedback loop is about 10 %.

In order to achieve full longitudinal coherence the radiation bandwidth $\Delta\lambda/\lambda$ fed back to the entrance of the undulator should correspond to $\lambda/\pi\sigma_z$ where σ_z is the rms length of the electron bunch (see Fig. 6). In this case the monochromatic photon pulse and the electron bunch would have the same length providing optimum seeding efficiency. In practice, however, the 1 ps long photon pulse should be stretched, i.e. the monochromator bandwidth should be further reduced, by a factor of about 4 in order to avoid a reduced overlap between electron and photon pulses due to a ± 1 ps time jitter. This requires a resolving power of the monochromator $\lambda/\Delta\lambda \simeq 2 \times 10^4$ at $\lambda = 120$ nm.

The narrow-band monochromator is made up by the plane grating in Littrow mounting [8,9] and the spherical mirror M_2 with a radius of 91.2 m which focuses the radiation on the entrance of the undulator. This simple arrangement requires only two optical components providing high throughput and continuous wavelength tuning just by rotating the grating. If no or only little wavelength tuning was required it would even be sufficient to use a spherical or toroidal grating as the only optical element. The distance between the mirrors M_2 and M_1 is 66.1 m, the distance between M_2 and the grating is 0.5 m. Thus, the feedback system re-injects the optical pulses after a delay of 444 ns, four times the electron bunch separation of 111 ns.

The principle of operation of the Littrow grating is illustrated in Fig. 7. For the central ray and the wavelength λ_0 for which the Littrow condition is exactly fulfilled, the angles α and β, respectively, of the incoming and the reflected beam with respect to the grating normal are identical. A high grating efficiency can be achieved by using sawtooth-shaped grooves such that reflection from the groove facets is specular (so-called blazed grating). This requires a blaze angle $\theta_B = \alpha = \beta$. The wavelength can be scanned by simply rotating the grating. The Littrow condition $\alpha = \beta$ is always fulfilled

in the present design, however, the blaze condition only holds for a single wavelength. In addition to the monochromatization of the radiation, the grating serves as a pulse stretcher (see Fig. 8) [9]. Each working groove in the grating causes the pulse to lengthen by one wavelength and increases the duration of the pulse.

The monochromator does not require entrance and exit slits. The central hole in the outcoupling mirror is the entrance slit and the electron beam itself with its small transverse size of 100 μm serves as the exit slit. Due to the given overall arrangement the source, i.e. the hole in the outcoupling mirror, is imaged into the focal plane crossing the electron beam at the undulator entrance with a demagnification of about 1:2 (35 m : 65 m, see Fig. 1). The groove density of the grating must be large enough to disperse the required bandwidth $\Delta\lambda$ at least as much as the size of that image. For the present geometry and a given wavelength λ this results in a groove width of the grating $d \simeq 3\lambda$. At 120 nm one can use a 2800 l/mm grating in first order. For shorter wavelengths it may be necessary to work in second or third order. The illuminated area of the grating is 15 mm (see Fig. 4) such that about twice as many grooves as the required resolving power for a given wavelength are covered. Hence, we do not run into the diffraction limit of the grating.

The optical aberrations of the feedback system have been estimated by using a simple geometrical ray tracing which did not include diffraction (except for the grating equation). Monochromatic radiation from a uniform, 1 mm $\times$ 1 mm square source at the position of the M_1 mirror was traced through the complete optical system up to an image plane at the entrance of the undulator (see Fig. 1). The angular distribution used for the source was somewhat larger than the diffraction from an aperture of the same size. Fig. 9a shows the images for three different photon energies using a 2400 l/mm grating in first order, and demonstrates both the high energy dispersion of the monochromator and the small contribution of aberrations. The latter can be estimated from the image of a monochromatic point source shown in Fig. 9b. The angular distribution of the point source as well as all other parameters were the same as those used for Fig. 9a. Aberrations affecting the energy resolution, such as coma and spherical aberrations, are negligible because all optical components are used near normal incidence and the beam divergence is diffraction limited. The dominating aberration is astigmatism blurring the image sagittally. This term can be kept small compared with the image size by choosing a sufficiently small deflection angle on mirror M_2. For the present study we have used a total deflection angle of 6^0. The separation between the meridional and the sagital focus is about 15 cm and is much smaller than the Rayleigh length (about 1.5 m).

The angular tolerances required for the monochromator adjustment and stability

are defined by the ratio of the electron beam radius and the distance to the undulator entrance and is thus of the order of a few microradians. This implies that also the surface slope errors of the mirror M_2 and the grating should be no larger than about 1 microradian. Such high quality mirrors and gratings are commercially available if their surfaces are plane or spherical. Overall the technical demands on the optical feedback system are quite similar to those on high resolution VUV monochromators used in many synchrotron radiation laboratories. If necessary. one could improve the stability by an active adjustment system as indicated in Fig. 3.

For maximum efficiency the grating surface should be made from a highly reflecting material such as SiC for the range between 200 nm (6.2 eV) and 60 nm (20.7 eV) or Pt for still shorter wavelengths down to 40 nm (31 eV). The normal incidence reflectivities of SiC and Pt in this energy range are plotted in Fig. 10. Since the on-blaze condition is only fulfilled for a single wavelength, it is necessary to use two or three gratings in order to cover the full energy range with high efficiency. This also allows to work near the optimum energy resolution by choosing the proper line density and order of diffraction for each grating. For example, two gratings, one with 2400 l/mm, the other with 3600 l/mm, could be used in first and second order, spanning the range from 200 nm to 60 nm in four steps with optimum energy resolution and efficiency. This is illustrated in Fig. 11 showing the diffraction efficiencies calculated for these two blazed gratings. From Figures 10 and 11 the overall optical transmission, R_m, of the feedback system, i.e. three mirror reflections times the diffraction efficiency of the grating, can be estimated to be around 1-5 % (see also the plot for R_m in Fig. 11).

3 Operation of the regenerative FEL amplifier

The regenerative FEL amplifier starts from shot noise and after the first pass the output radiation has the usual SASE properties [10]. For the parameters of the Phase I TTF FEL the effective power of shot noise is a few watts. The dependence of the expected SASE output radiation power after the first pass on the undulator length has been calculated for different electron beam qualities and is presented in Figs. 12–14.

Let us consider in detail the specific example of the FEL amplifier operating at a wavelength of 120 nm driven by an electron beam with 4π mm mrad normalized emittance and 250 keV energy spread. The undulator length is 13.5 m and the external focusing beta function is 1.2 m. In this example the effective power of shot noise at the undulator entrance is about 2.5 W. Using Fig. 13 we obtain that the output radiation power after the first pass is equal to 300 MW.

For effective operation of the regenerative FEL amplifier the input power delivered to its entrance by the feedback should exceed significantly the shot noise power. Let us estimate the input radiation power delivered to the undulator entrance at the second pass. The feedback transmission factor can be written as $T_{\rm fb} = K_{\rm coup} R_{\rm m} K_{\rm s}$, where $K_{\rm coup} \simeq 10^{-1}$ is the fraction coupled out through the hole in mirror M_1, $R_{\rm m} \simeq 4 \times 10^{-2}$ is the integral reflection coefficient of the mirrors and the dispersive element (see Fig. 11), and $K_{\rm s}$ refers to the losses due to the spectral dispersion:

$$K_{\rm s} = \frac{(\Delta\lambda/\lambda)_{\rm m}}{(\Delta\lambda/\lambda)_{\rm SASE}} \simeq 5 \times 10^{-3}.$$

Here $(\Delta\lambda/\lambda)_{\rm m} \simeq 5 \times 10^{-5}$ is the monochromator bandwidth and $(\Delta\lambda/\lambda)_{\rm SASE} \simeq 10^{-2}$ is the radiation bandwidth of the SASE FEL. In addition, the grating reduces the peak power of the coherent input signal further since it stretches the pulse longitudinally by a factor of 4.

Finally, the radiation from the feedback loop is focused on the electron beam at the undulator entrance. Here we have to take into account the imperfect lateral overlap between the focused monochromatic radiation and the electron bunch at the undulator entrance which will lead to an additional loss of input radiation power. A quantitative description of this effect may be performed in the following way. We assume that the seed radiation has a Gaussian radial intensity distribution which is characterized by the position of the focus, z_0, and the size of the waist in the focus, w. At the focus, $z = z_0$, the Gaussian beam has a plane phase front and a Gaussian distribution of the amplitude:

$$E(r, z_0) = E_0 \exp\left(-\frac{r^2}{w^2}\right) .$$

In the high gain linear regime the radiation power grows exponentially:

$$G = A \exp\left[2{\rm Re}(\Lambda) z\right],$$

where Λ is the eigenvalue of the ground mode TEM_{00} which has the highest gain. The preexponential factor A depends on the focusing of the seed radiation and is a function of z_0 and w. It should be maximized by an appropriate choice of w and z_0. This problem has been studied in detail in paper [11] using the solution of the initial-value problem. It has been found that the result of the optimization does not depend significantly on the position of the Gaussian beam waist and it can be placed at the coordinate of the undulator entrance, $z_0 = z_{\rm ent}$. Fig. 15 presents the dependence of the preexponential factor A on the reduced Gaussian beam waist $\hat{w} = w/\sigma$, where σ is the r.m.s. transverse electron beam size. The FEL amplification process has been

calculated using the 2-D steady-state code FS2R [11,12].

In the present design the lateral size of the photon beam focus, w, is completely determined by the fixed geometry of the feedback optical system (i.e. the size of the hole in the out-coupling mirror, the focal distances of the mirrors and the distances between the optical elements). The transverse size of the electron beam in the undulator, σ, is also fixed since it is defined by the design of the accelerator and the undulator. In our numerical example for $\lambda = 120$ nm the size of the photon beam focus is about $w \simeq 0.5$ mm which is four times larger than the rms electron beam size, σ. On the other hand, optimum overlap of the photon and electron pulses requires a ratio $w/\sigma \simeq 1.3$ (see Fig. 15). Such a mismatch, however, is not dramatic and will result in a reduction of the input power by a factor of 4 only.

Taking into account all the effects mentioned above, the overall loss factor for the feedback system is about 1.2×10^{-6}. As a result, the injected power delivered to the undulator entrance at the second pass is about 350 W. The effective power of shot noise is about 2.5 W and is much smaller than the coherent signal. Thus, after the first pass the RAFEL amplifies coherent seed radiation.

In this section we have presented a specific numerical example for the regenerative FEL amplifier working at a wavelength of 120 nm. However, we would like to emphasize that the wavelength can be tuned continuously by changing the electron beam energy and adjusting the monochromator wavelength by a simple rotation of the grating. Using SiC-coated optical elements it should be possible to cover the range from $\sim$ 200 nm down to $\sim$ 60 nm (see Fig. 11).

4 Simulation of the second harmonic generation

In order to obtain shorter wavelengths, the present RAFEL design can be easily upgraded by an additional short undulator for harmonic generation installed behind the main undulator. The electron pulse at the exit of the main undulator is bunched and the density modulation of the electron pulse contains multiple harmonics of the main frequency. Tuning the fundamental frequency of the short undulator to the second harmonic of the main undulator will allow one to reach wavelengths down to $\sim$ 30 nm. Simulation of harmonic generation has been performed using the TDA3D code [13,14]. In the simulations, two different beam qualities have been assumed by changing the longitudinal velocity spread. One set corresponds to a normalized emittance of 2π mm mrad and an energy spread of 500 keV, the second to an emittance of 4π mm mrad and an energy spread of 250 keV. Figs. 16–18 show the results for a superconducting helical undulator with a period of 13 mm. The maximum power that can be achieved

decreases rapidly with increasing distance between main undulator and radiator due to debunching caused by the large energy spread. Saturation occurs at a radiator length of approximately 1.5 m, as shown in Fig. 18. Note the difference between Fig. 16 and 17, where the feedback fraction has been changed from 10^{-4} to 10^{-6}, resulting in a significantly higher saturation power without changing the length of the radiator. For a larger reduction in feedback power the feedback system would effectively seize to exist, since the power would become comparable to the shot noise power. For a conventional planar undulator with a 20 mm long period, the saturation length increases to 2 m (see Fig. 19). With a distance between main undulator and radiator of less than 1 m, the peak power of the second harmonic is of the order of a few megawatts, approximately two orders of magnitude below the saturation power of the fundamental frequency. The average output power of the second harmonic will be still high enough, about a fraction of watt.

Acknowledgements

We wish to thank P. Gürtler, T. Limberg, G. Materlik, T. Möller, U.-K. Müller, C. Pagani, J. Pflüger, J. Roßbach, J.R. Schneider, S. Schreiber, B. Sonntag and H. Weise for useful discussions. We are grateful to U. Hahn, J. Halik, A. Kabel and W. Sobala for technical support.

References

[1] J. Feldhaus et al., Nucl. Instrum. and Methods **A393**(1997)162.

[2] J. Feldhaus et al., Optics Commun. **140**(1997)341.

[3] J. Feldhaus et al., Proc. SPIE **2988**(1997)145.

[4] B. Adams and G. Materlik, Proc. XVIII Int. FEL Conference (Rome, 1996), p.II-24.

[5] B. Adams, Proc. XVIII Int. FEL Conference (Rome, 1996), p.II-26.

[6] W. Brefeld et al., Nucl. Instrum. and Methods **A393**(1997)119.

[7] J. Goldstein, D. Nguyen and R. Sheffield, Nucl. Instrum. and Methods **A393**(1997)137.

[8] M.C. Hutley, "Diffraction gratings" (Academic Press, London, 1982).

[9] J. Sollid et al., Nucl. Instrum. and Methods **A285**(1989)147.

[10] E.L. Saldin, E.A. Schneidmiller and M.V.Yurkov, "Statistical properties of radiation from VUV and X-ray free electron laser", DESY print TESLA-FEL 97-02, Hamburg, 1997. Optics Communications, in press.

[11] E.L. Saldin, E.A. Schneidmiller and M.V.Yurkov, Optics Commun. **97**(1993)272.

[12] E.L. Saldin, E.A. Schneidmiller and M.V.Yurkov, Optics Commun. **95**(1993)141.

[13] T.-M. Tran and J.S. Wurtele, Comp. Phys. Commun. **54**(1989)263.

[14] P. Jha and J.S. Wurtele, Nucl. Instrum. and Methods **A331**(1993)477.

[15] F. Schäfers and M. Krumrey, BESSY Technical Report TB 201/96, 1996.

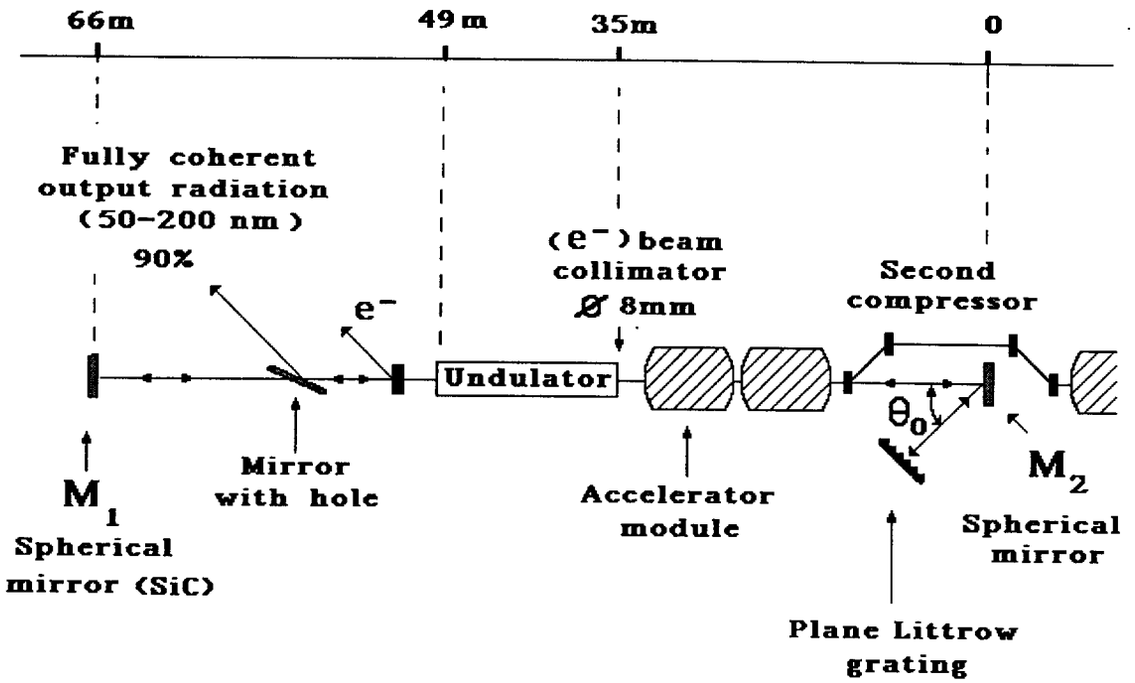

Fig. 1. Schematic layout of the UV-VUV regenerative FEL amplifier at the TESLA Test Facility.

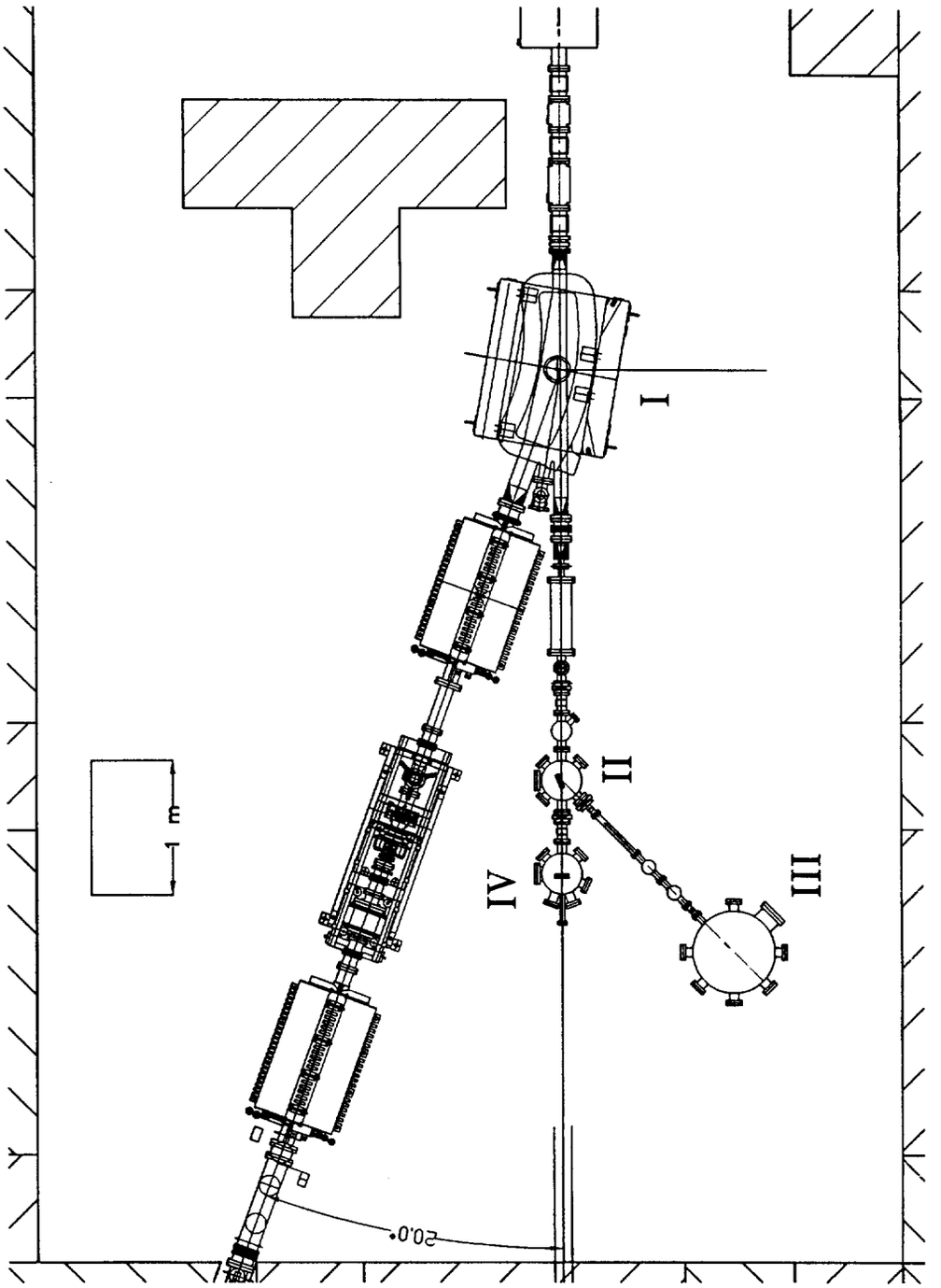

Fig. 2. The experimental area. The spectrometer magnet (I) separates the electron beam from the photon beam and the plane mirror (II) reflects most of the radiation into the experiment (III). Approximately 10% of the radiation is leaking through a $\sim$ 1 mm hole in the plane mirror and is backscattered by a spherical mirror (IV) towards the monochromator (see Fig. 1).

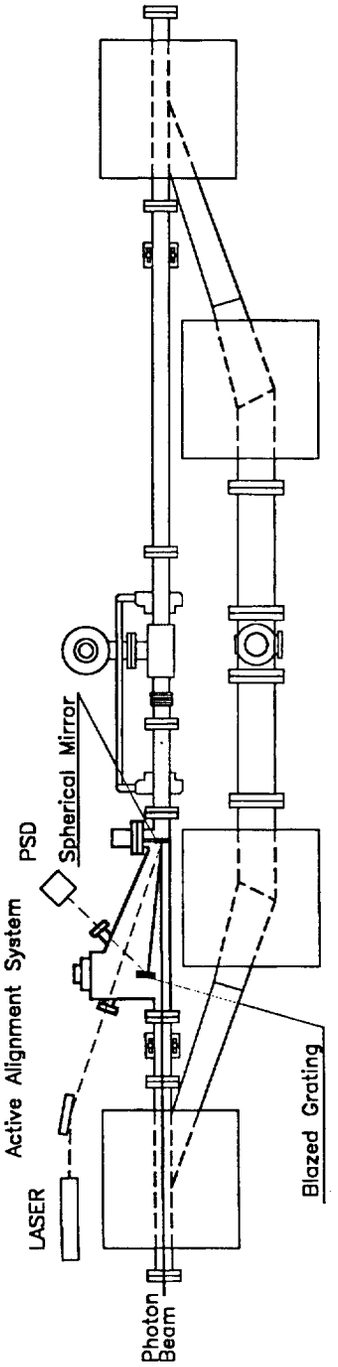

Fig. 3. Layout of the monochromator in the second bunch compressor.

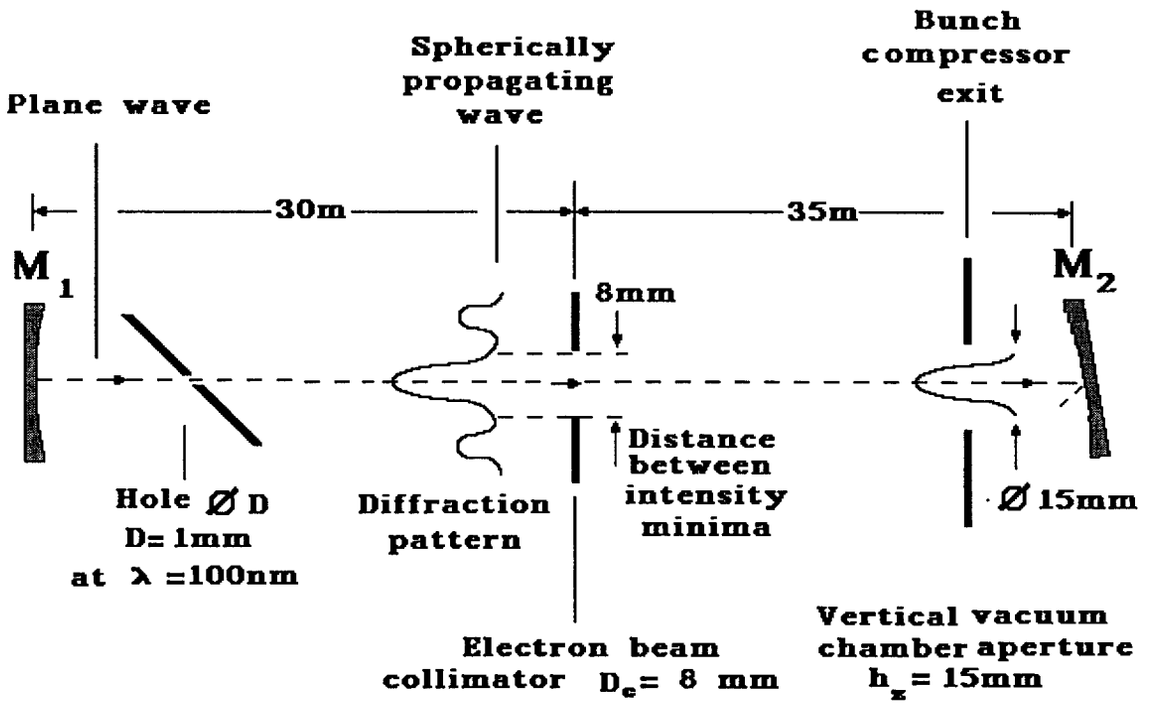

Fig. 4. Determination of the mirror hole diameter for the feedback system.

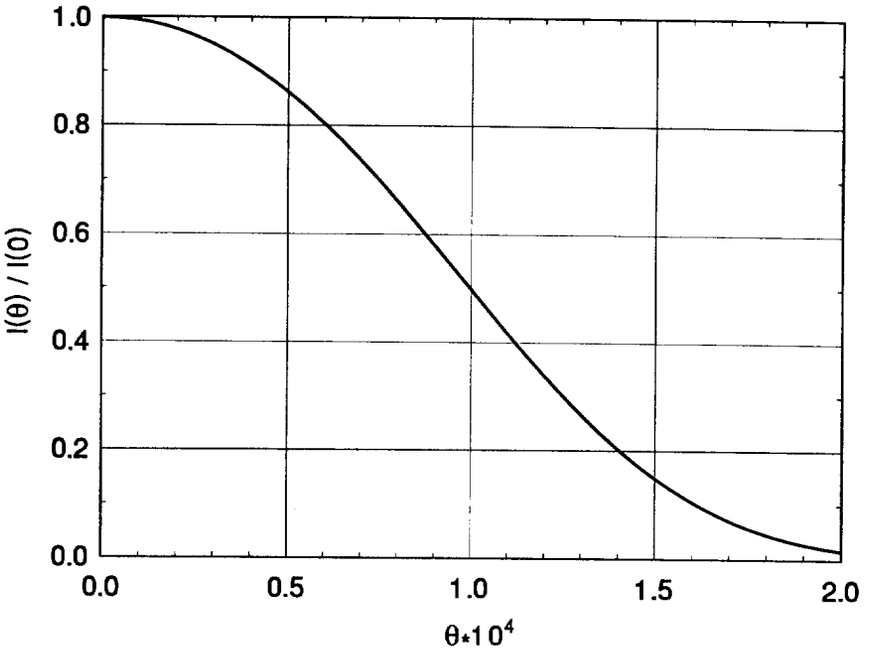

Fig. 5. Directivity diagram of the 120 nm radiation from the FEL amplifier operating at saturation for a normalized emittance of 4π mm mrad and an energy spread of 250 keV.

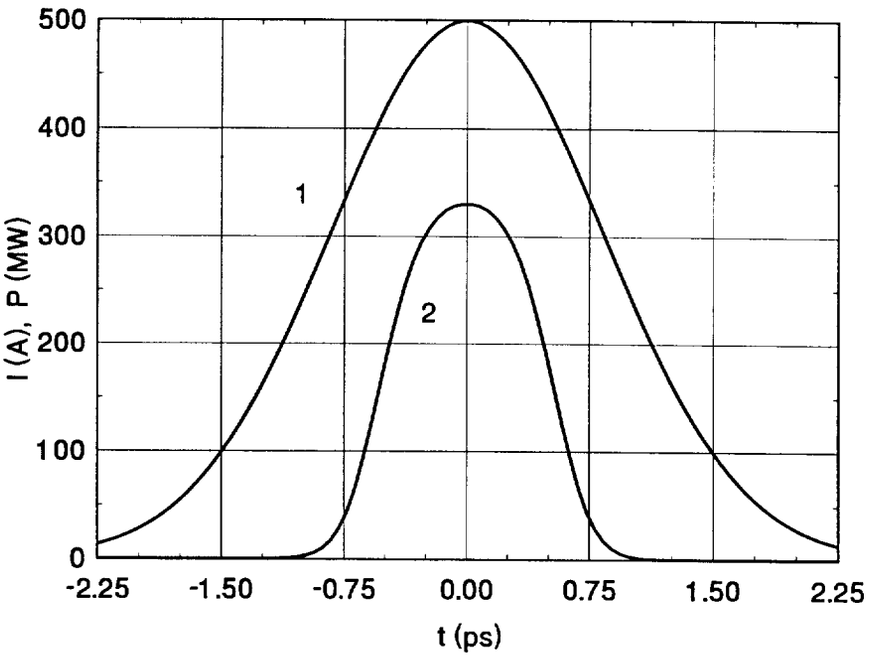

Fig. 6. Time dependence of the electron bunch current (curve 1) and of the FEL radiation power at saturation (curve 2) for a wavelength 120 nm, a normalized emittance of 4π mm mrad and an energy spread of 250 keV.

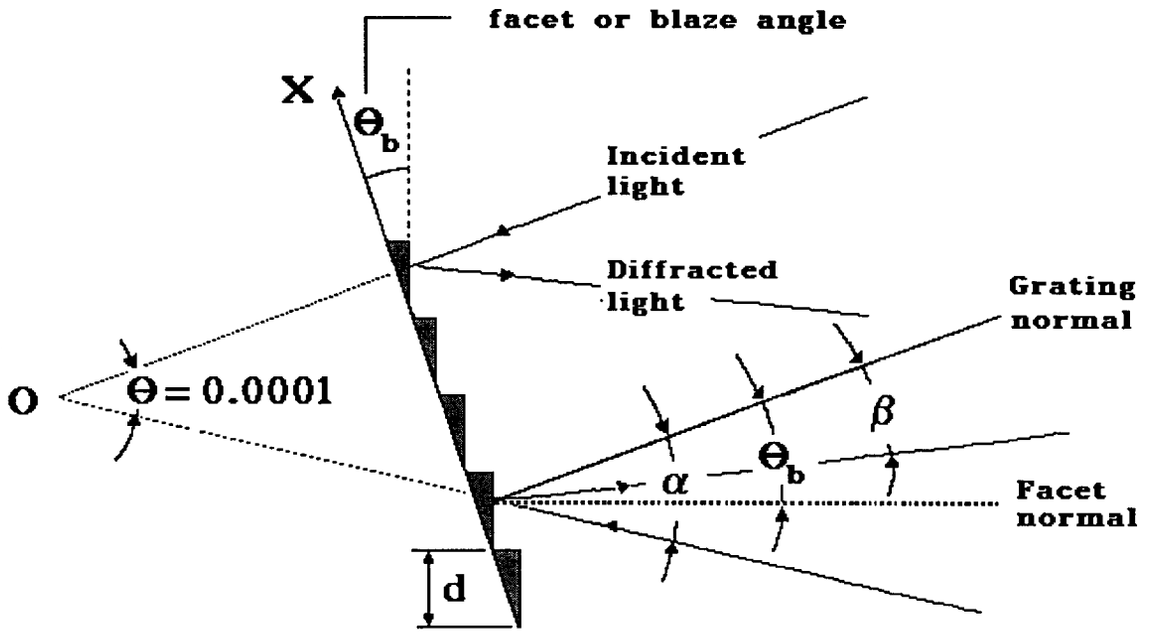

$$\sin\alpha + \sin\beta = \lambda/d \simeq 2\sin\Theta_b$$

Fig. 7. Illumination of the Littrow grating.

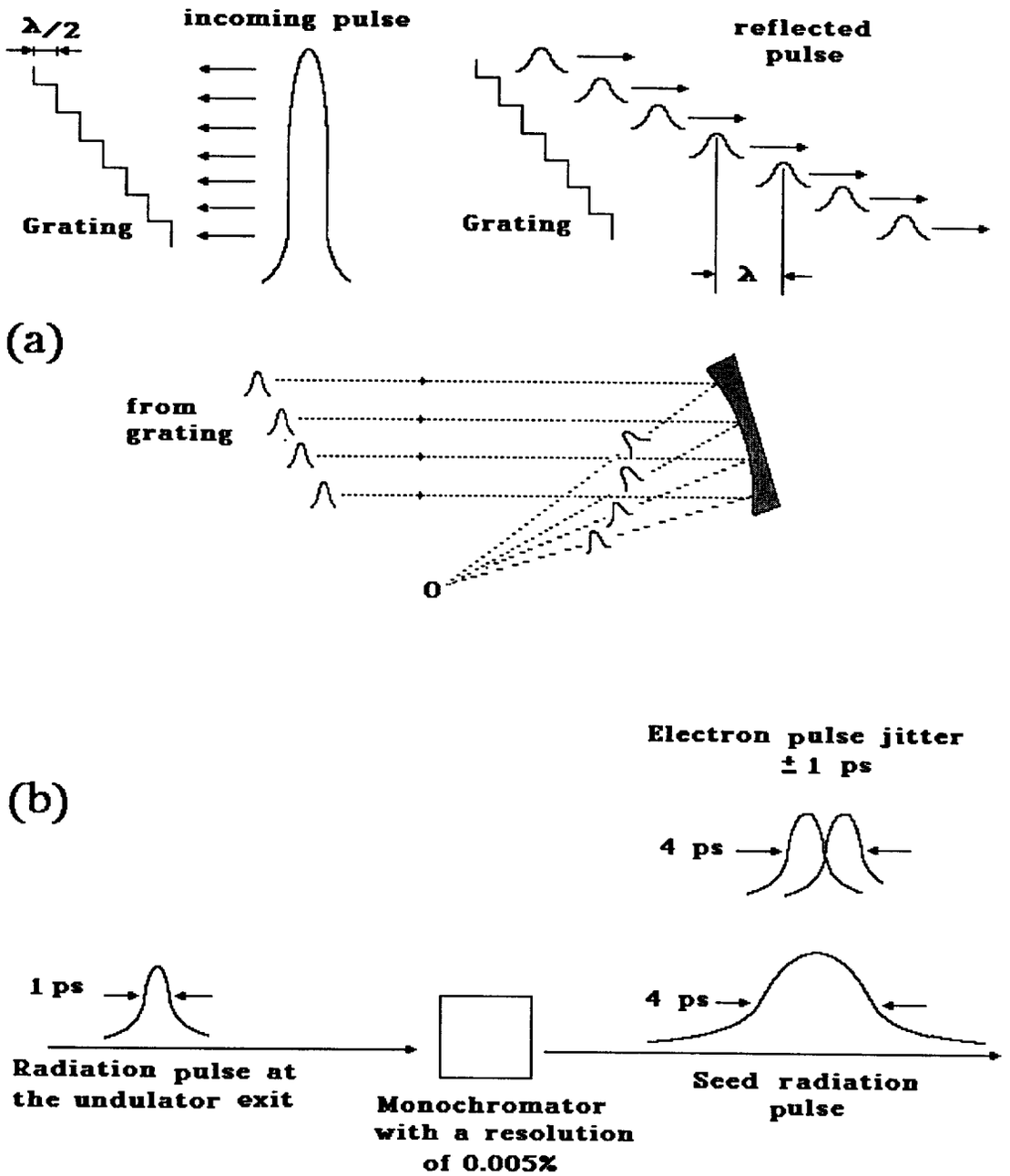

Fig. 8. The use of a Littrow grating as a pulse stretcher. Drawing (b) illustrates how electron pulse jitter effects on the feedback system can be avoided.

(a)

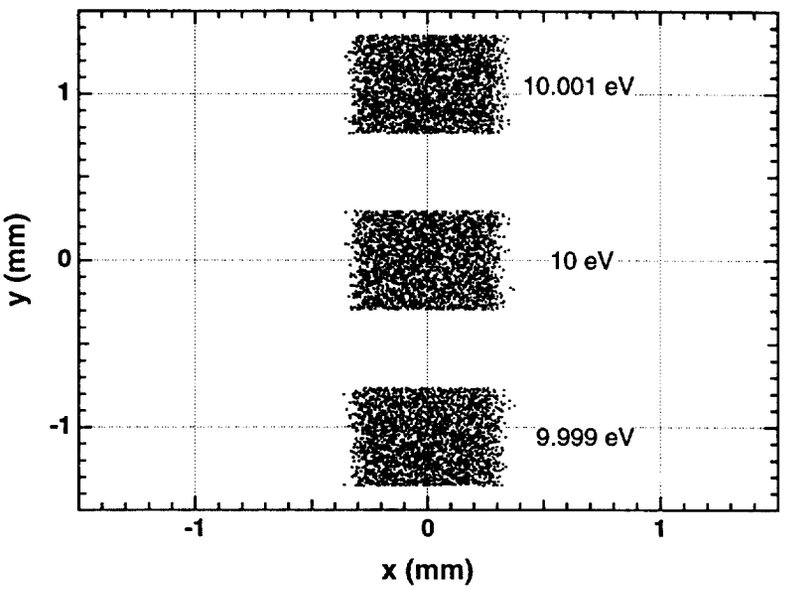

(b)

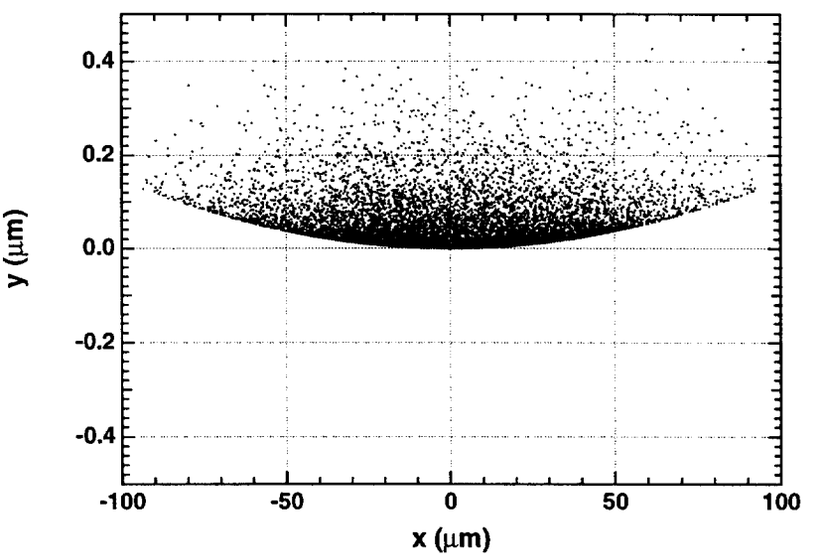

Fig. 9. Raytracing through the optical system shown in Fig. 1. (a): Image of a 1×1 mm square source for photon energies of 9.999 eV, 10 eV and 10.001 eV showing the large energy dispersion and the small aberrations of the optics. (b): Image of a monochromatic point source ($h\nu = 10eV$) with the same angular divergence indicating the contribution of optical aberrations.

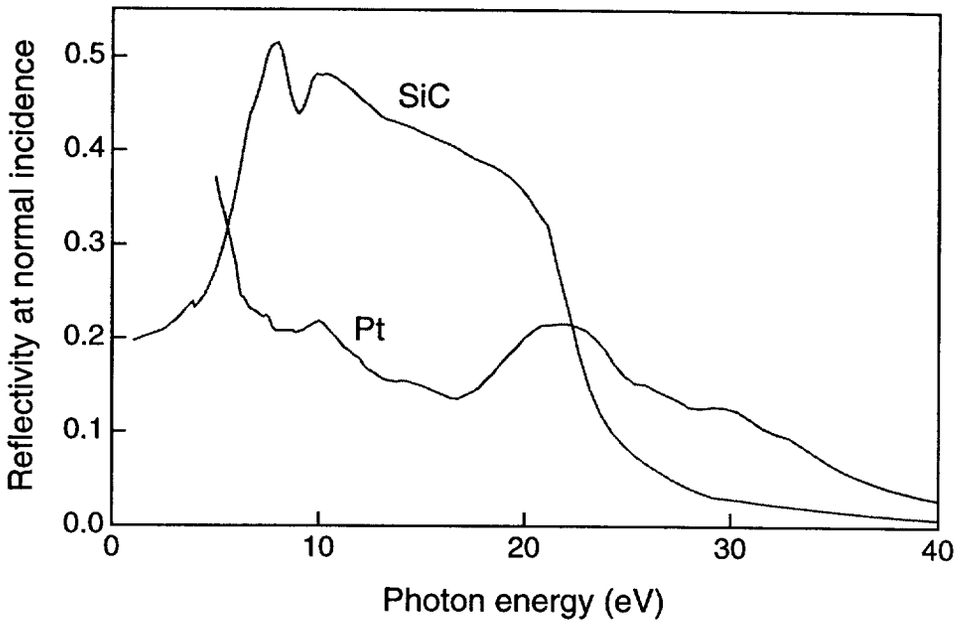

Fig. 10. Reflectivity of SiC and Pt at normal incidence calculated from the optical constants using REFLEC [15].

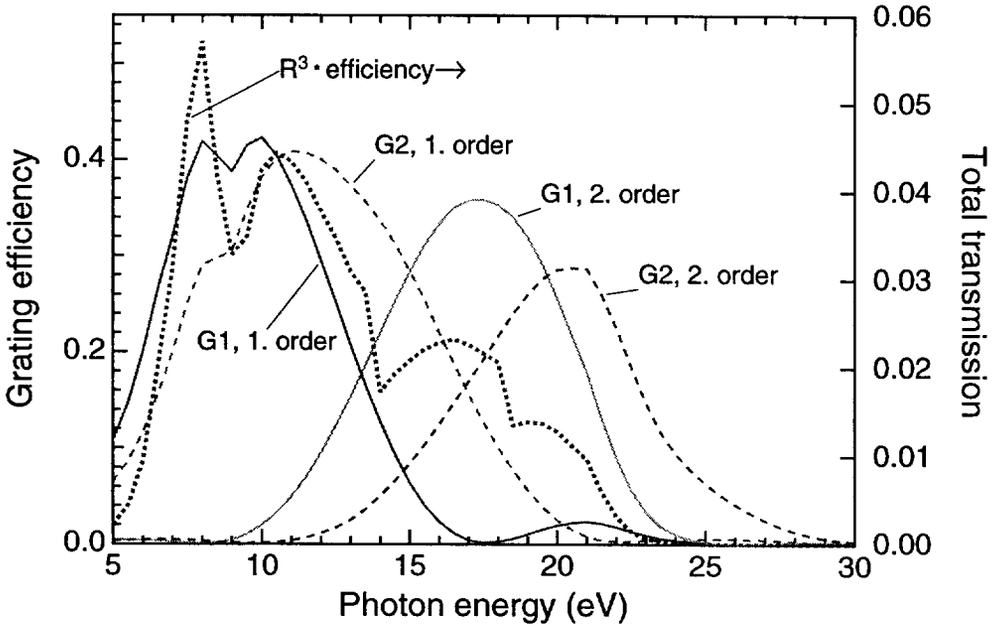

Fig. 11. Efficiency of two blazed SiC gratings for s-polarized light in first and second order calculated with REFLEC [15]. The grating G1 (full lines) has 2400 l/mm and a blaze angle of 10^0, grating G2 (dashed lines) has 3600 l/mm and a blaze angle of 12^0. The dotted curve represents the total transmission, R_m, of the optical system and is the product of the reflectivity of three SiC mirrors and the efficiency of the grating that should be used at a certain energy.

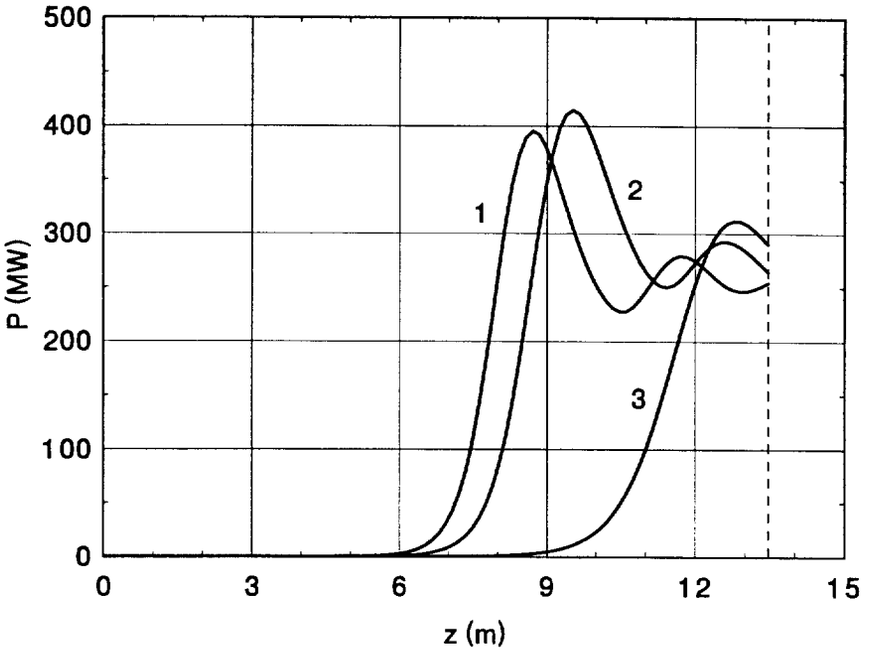

Fig. 12. Dependence of the radiation power on the undulator length for 120 nm wavelength, a normalized emittance of 2π mm mrad and an effective power of shot noise of 4 W. The energy spread is 100 keV (curve 1), 250 keV (curve 2) and 500 keV (curve 3).

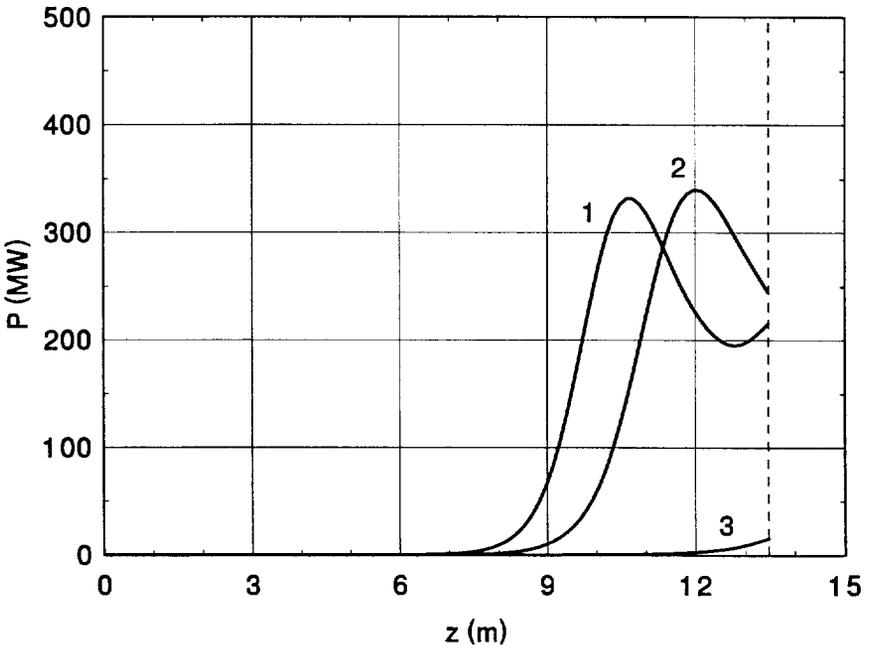

Fig. 13. Dependence of the radiation power on the undulator length for 120 nm wavelength, a normalized emittance of 4π mm mrad and an effective power of shot noise of 2.5 W. The energy spread is 100 keV (curve 1), 250 keV (curve 2) and 500 keV (curve 3).

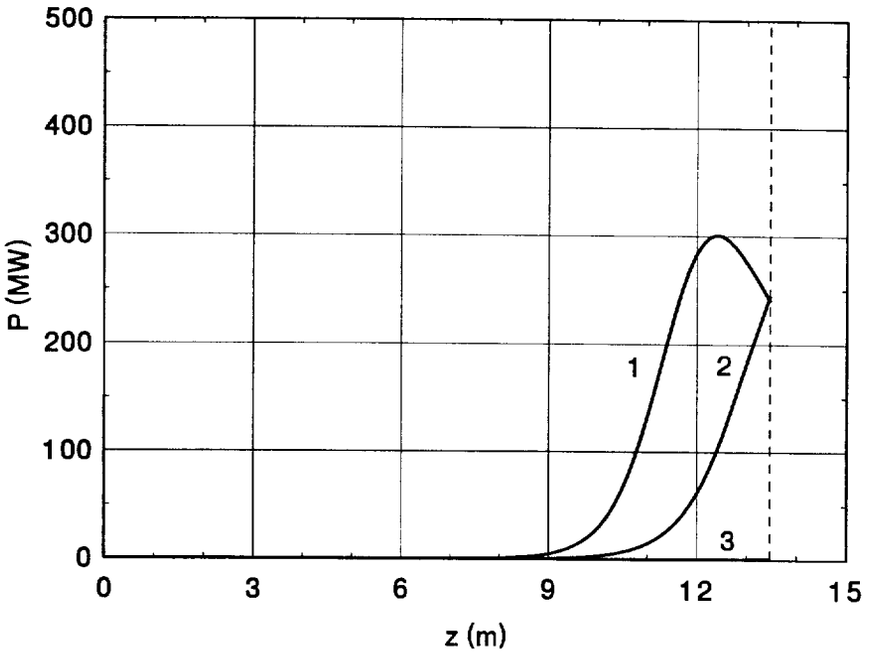

Fig. 14. Dependence of the radiation power on the undulator length for 120 nm wavelength, a normalized emittance of 6π mm mrad and an effective power of shot noise of 2 W. The energy spread is 100 keV (curve 1), 250 keV (curve 2) and 500 keV (curve 3).

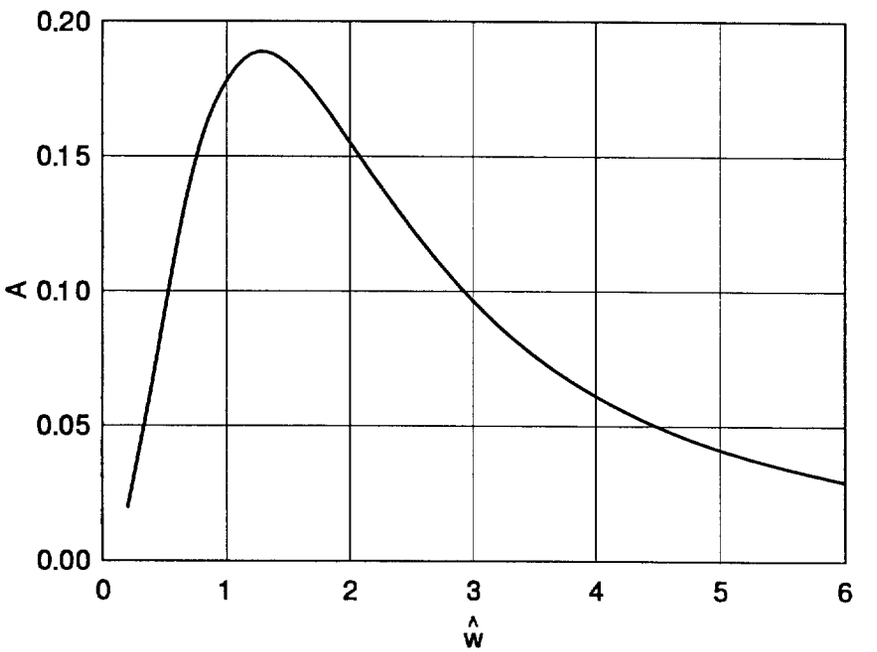

Fig. 15. Dependence of the preexponential factor A on the reduced waist of the input optical beam. Here the wavelength is 120 nm, the normalized emittance is 4π mm mrad and the energy spread is 250 keV.

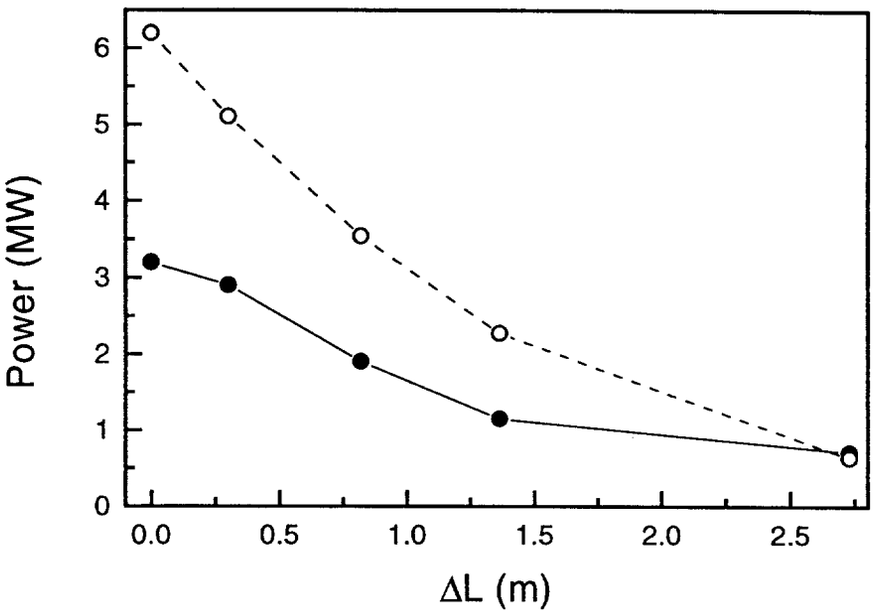

Fig. 16. Power of the second harmonic at 60 nm in a 1.5 m long radiator (helical superconducting undulator with a 13 mm period) as a function of the distance between the exit of the main undulator and the radiator entrance. The power fraction returned to the entrance of the main undulator is 10^{-4}. The open symbols represent results with an initial energy spread of 250 keV and a normalized emittance of 4π mm mrad, the solid circles with 500 keV and a normalized emittance of 2π mm mrad.

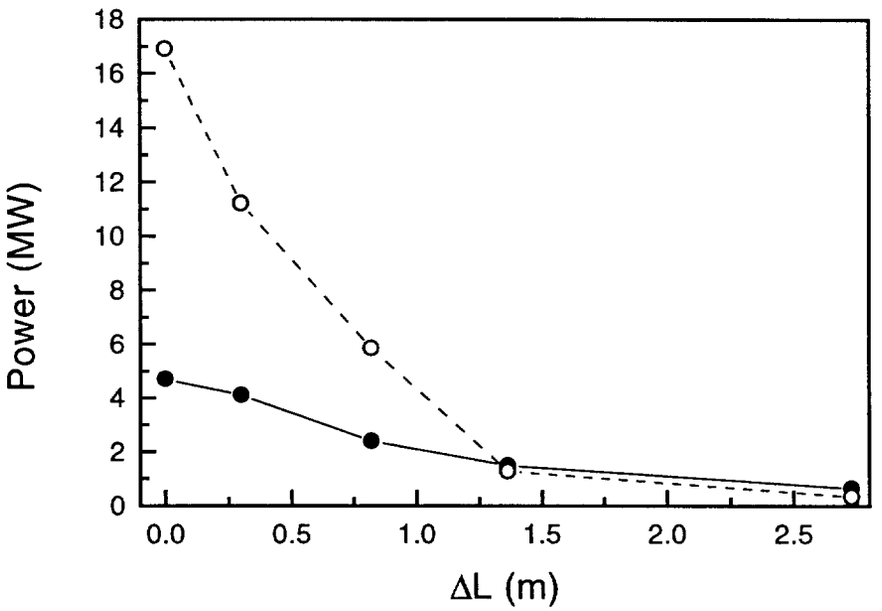

Fig. 17. Power of the second harmonic at 60 nm in a 1.5 m long radiator (helical superconducting undulator with a 13 mm period) as a function of the distance between the exit of the main undulator and the radiator entrance. The power fraction returned to the entrance of the main undulator is 10^{-6}. The open symbols represent results with an initial energy spread of 250 keV and a normalized emittance of 4π mm mrad, the solid circles with 500 keV and a normalized emittance of 2π mm mrad.

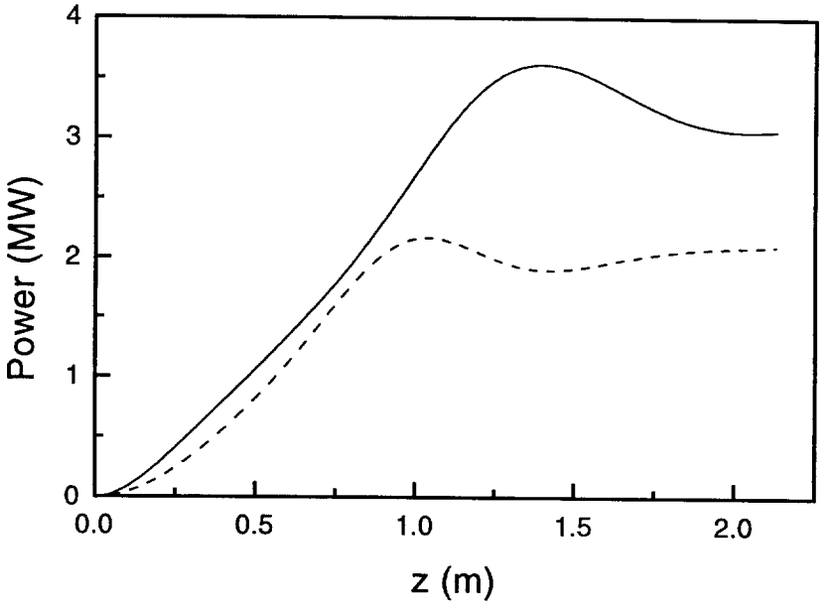

Fig. 18. Power growth of the second harmonic at 60 nm along the radiator (helical superconducting undulator with a period of 13 mm) placed at a distance of 0.82 m from the main undulator. The power fraction returned to the entrance of the main undulator is 10^{-4}. The dashed line represents results with an initial energy spread of 250 keV and a normalized emittance of 4π mm mrad, the solid line with 500 keV and a normalized emittance of 2π mm mrad.

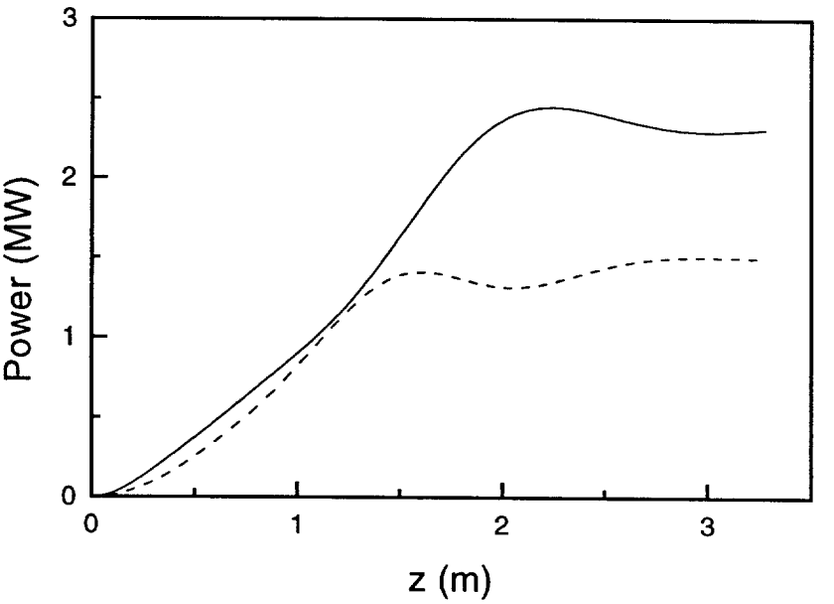

Fig. 19. Power growth of the second harmonic at 60 nm along the radiator (permanent magnet undulator with a 20 mm period) placed at a distance of 0.82 m from the main undulator. The power fraction returned to the entrance of the main undulator is 10^{-4}. The dashed line represents results with an initial energy spread of 250 keV and a normalized emittance of 4π mm mrad, the solid line with 500 keV and a normalized emittance of 2π mm mrad.